

Borane-functionalized silica supports In situ activated heterogeneous zirconocene catalysts for MAO-free ethylene polymerization

Sumate Charoenchaidet^a, Sumaeth Chavadej^a, Erdogan Gulari^{b,*}

^a The Petroleum and Petrochemical College, Chulalongkorn University, Bangkok 10300, Thailand

^b Department of Chemical Engineering, University of Michigan, Ann Arbor, MI 48109-2136, USA

Received 22 October 2001; received in revised form 10 December 2001; accepted 10 December 2001

Abstract

We treated silica with tris(pentafluorophenyl)borane, $B(C_6F_5)_3$, to create borane-functionalized support, $SiO_2-B(C_6F_5)_3$ which was then used as a support and co-catalyst for the in situ activated dichloro-zirconocene ($Cp_2ZrCl_2/TIBA$) and dimethyl-zirconocene catalyst systems ($Cp_2Zr(CH_3)_2$) for ethylene polymerization. The surface modifications of $SiO_2-B(C_6F_5)_3$ was investigated by SEM-EDX, FTIR and XPS to determine the distribution of fluorine and boron atoms on the silica surface as a measure of the presence of $B(C_6F_5)_3$ and interaction with the siloxane groups of the silica support. Catalytic performances are presented in the form of ethylene consumption rate profiles. The results show that the independent of the time dedicated to the in situ activation of the metallocene, all pre-activated systems showed activity decay. In contrast, the in situ activated systems either showed little or no activity decay. The presence of TIBA was adequate to make an active MAO-free catalyst system. The pre-activated and in situ activated metallocene systems produced polyethylene with slightly different molecular weights (MWs) and molecular weight distribution (MWD). MWDs were quite narrow ~ 3 . The bulk density of polyethylene product is highest for the in situ activated metallocenes, but there is no difference between the products of dichloro- and dimethyl-zirconocenes. Pre-activated and in situ activated catalysts show no reactor fouling. © 2002 Elsevier Science B.V. All rights reserved.

Keywords: Ethylene polymerization; Zirconocene catalyst; Borane; Supported metallocene; In situ activated catalyst

1. Introduction

Metallocene catalysts have revolutionized olefin polymerization catalysis because of improved polymers properties. When compared to conventional Ziegler–Natta catalysts, they provide high activity and narrow molecular weight distribution (MWD).

Moreover, these catalysts also result in lower residual metal content in final product. Heterogeneous metallocene systems have an advantage over homogeneous metallocene systems because of easy adaptation to use in the existing industrial polymerization processes (*drop-in technology*) by a simple exchange with the conventional Ziegler–Natta catalysts. Other advantages when compared to homogeneous metallocene systems are: avoiding the “fouling-effect”, the sticking of formed polymer to the reactor wall, good controllable morphology and high bulk density of polymer products [1–3].

* Corresponding author. Tel.: +1-734-763-5941;

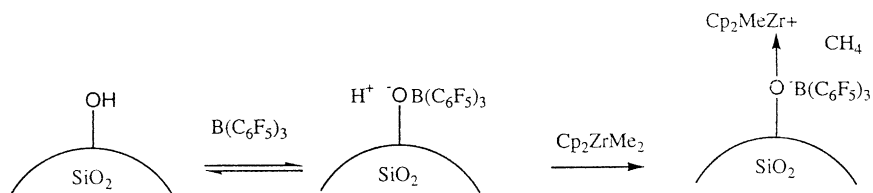
fax: +1-734-763-0459.

E-mail address: gulari@engin.umich.edu (E. Gulari).

In general, heterogeneous metallocene catalysts have a lower catalytic activity than their corresponding homogeneous metallocene systems. There are two main reasons for the decrease in activity: (1) steric hindrances of active species on the support surface during polymerization and (2) deactivation of active metal sites during the supporting process [1].

Highly active heterogeneous metallocenes can be developed by using novel active materials for impregnation as support. Various silicas have been used as the most general support to immobilize metallocene compounds on its surface. Other inert supports for this propose, such as silica gel, alumina, magnesium chloride, starch, zeolite and polymer beads, have also been reported in the literature [2,3]. There are

been developed for activation of metallocenes and to generate equilibrium concentrations of the catalytically active species $[\text{Cp}_2\text{MR}]^+$ [7]. The immobilization of the active $\text{B}(\text{C}_6\text{F}_5)_3$ on silica supports was suggested. This process involved the conversion of surface OH groups into $-\text{OB}(\text{C}_6\text{F}_5)_3$ anions [8]. This supported co-catalyst can generate an active cationic species “metallocenium” $[\text{Cp}_2\text{ZrMe}]^+$ because the anionic borane remains adducted to the support by electrostatic forces without anchoring via a covalent tether [9,10]. Tian et al. [8] studied the functionalization of $\text{B}(\text{C}_6\text{F}_5)_3$ on partially hydroxylated silica and fully hydroxylated alumina. The reaction mechanism of borane functionalized or supported zirconocene on silica is proposed to be



several approaches for creating a heterogeneous metallocene: (1) impregnation of metallocene catalysts onto those supports directly without treating the support with alkylaluminum compounds; (2) forming a chelating ligand on the support followed by contact with the metal salt; (3) immobilization of methylaluminoxane (MAO) on the support followed by reacting with a metallocene. This last method can provide high-performance catalysts while reducing the use of MAO and additional alkylaluminum compounds. These catalyst systems are active for olefin polymerization, particularly in the context of gas-phase polymerization processes or in slurry polymerization in the presence of alkylaluminum compounds [2].

In order to avoid the complexity of a separate catalyst preparation step, in situ metallocene activation technique on a support before polymerization was developed [4,5], using $\text{Et}[\text{Ind}]_2\text{ZrCl}_2$ catalyst and MAO co-catalyst. The catalyst showed good catalytic activity. In addition, it produced polyethylene and ethylene-1-hexene copolymer with good morphology and high bulk density without fouling problems [4–6].

To reduce the large amount of MAO required as a co-catalyst, weakly coordinating organoboron compounds such as tris(perfluorophenyl)borane ($\text{B}(\text{C}_6\text{F}_5)_3$) and tetrakis(perfluorophenyl)borate ($(\text{C}_6\text{F}_5)_4\text{B}^+$) have

These borane-supported systems were shown to be active in the presence of low amount of MAO for ethylene polymerization [8]. However, the borane-supported silica can also result in a low activity, because the binding of $\text{B}(\text{C}_6\text{F}_5)_3$ to the surface hydroxyl groups can be reversible to $\text{Cp}_2\text{Zr}(\text{CH}_3)^+\text{B}(\text{C}_6\text{F}_5)_3^-$ when washing with toluene during the preparation [10]. This is due to the high solubility of $\text{B}(\text{C}_6\text{F}_5)_3$ in toluene. Other organic solvents have been suggested as being preferable such as the hexane used for this work.

Carney and Shih [11] developed the heterogeneous borate catalysts involved in the modification of the silica surface by replacing isolated hydroxyl groups with reactive hydrosilanes. This surface-modified silica was then reacted with a weak acid such as an alcohol by tethering with alkoxy silanes borate ($[\text{OH}-\text{Ph}-\text{B}(\text{C}_6\text{F}_5)_3]^- [\text{HNMe}_2\text{Ph}]^+$). The supported product was ready to activate dialkyl-metallocenes, and dichloro-metallocene when combined with an alkylaluminum and followed by the addition of anilinium borate. This catalyst system produced polyethylene with high molecular weight (MW), narrow MWD and high bulk density.

However, all the above-mentioned methods of catalyst preparation were completed by using alkyl

metallocenes and required an impregnation process of metallocene on the supports. In this paper, we report the results of our studies with in situ activated zirconocene systems such $\text{Cp}_2\text{ZrCl}_2/\text{TIBA}$, $\text{Cp}_2\text{Zr}(\text{CH}_3)_2$ on $\text{B}(\text{C}_6\text{F}_5)_3\text{-SiO}_2$. We also investigated the role of alkylaluminum TIBA.

2. Experimental

2.1. Materials

Polymerization grade ethylene and UHP grade nitrogen (Cryogenic, MI) were dried by passing through a column of oxygen-moisture trap (MATHESON). Tris(pentafluorophenyl)borane ($\text{B}(\text{C}_6\text{F}_5)_3$) solution (11 wt.% in toluene) was obtained from Albemarle. Silica gel (DavisilTM, grade 644, W.R. Grace, MA) used in this research has a surface area of $300\text{ m}^2/\text{g}$, and pore volume $1.15\text{ cm}^3/\text{g}$. Bis(cyclopentadiene)zirconiumdichloride (Cp_2ZrCl_2), bis(cyclopentadiene)zirconium dimethyl ($\text{Cp}_2\text{Zr}(\text{CH}_3)_2$) and triisobutylaluminum (TIBA, solution 1.0M in toluene) were purchased from Aldrich. Toluene (Aldrich, anhydrous grade, $\text{H}_2\text{O} < 0.001\%$) was refluxed with sodium for 48 h, then degassed by distillation under N_2 with CaH_2 reflux. Hexane (Aldrich, anhydrous grade, $\text{H}_2\text{O} < 0.002\%$) was bubbled with N_2 . All solvents were stored over molecular sieves before use.

2.2. Catalyst preparation

2.2.1. Support treatment

To prepare the partially hydroxylated silica, silica gel support was washed with DI-water and then dried at 50°C under vacuum. Then the support was packed into a horizontal quartz tube and dried at 500°C under oxygen flow for 6 h, and then cooled down with nitrogen flow to room temperature and stored under vacuum until use. The hydroxyl group content was approximately 1.42 OH mmol/g silica, determined by titration method with trimethylaluminum [12].

2.2.2. Preparation of $\text{B}(\text{C}_6\text{F}_5)_3\text{-SiO}_2$

All of the catalyst preparation steps were carried out under anhydrous and anaerobic conditions in a glove box (O_2 and $\text{H}_2\text{O} < 1\text{ ppm}$). The treated silica

gel (2 g), $\text{B}(\text{C}_6\text{F}_5)_3$ (3 ml in toluene or 0.63 mmol) and extra toluene (17 ml) were mixed together into a 100 ml of volumetric flask and refluxed for 12 h. Afterwards, the solids in the mixture were allowed to precipitate overnight before collecting only the solid part with a medium fritted funnel and washing with toluene ($3 \times 5\text{ ml}$) and hexane ($2 \times 5\text{ ml}$). The product was dried under vacuum for 4 h to afford 2.06 g of off-white solid.

2.2.3. Preparation of pre-activated metallocene catalyst

First, a mixture of Cp_2ZrCl_2 (1.6 μmol) and TIBA (1 mmol) in toluene (5 ml) was prepared. The desired amount of $\text{B}(\text{C}_6\text{F}_5)_3\text{-SiO}_2$ was placed in a 100 ml flask, and the premixed zirconocene solution was added. After stirring vigorously for 5 min at room temperature, the mixture was transferred to the reactor immediately for testing its polymerization activity in batch mode.

2.2.4. Preparation of in situ activated metallocene catalyst

Stock solutions of Cp_2ZrCl_2 (1.6 μmol)/TIBA (1 mmol) in toluene and $\text{Cp}_2\text{Zr}(\text{CH}_3)_2$ (20 μmol)/TIBA (1 mmol) in toluene, and the $\text{B}(\text{C}_6\text{F}_5)_3\text{-SiO}_2$ in toluene (5 ml) were prepared. First, a desired amount of zirconocene catalyst was added into the reactor. Following the slurry solution of $\text{B}(\text{C}_6\text{F}_5)_3\text{-SiO}_2$ was charged separately into the reactor. The zirconocene reacted directly inside the reactor with the silica-supported borane.

2.3. Polymerization system and procedures

The ethylene polymerization was carried out in a 500 ml stainless steel reactor (Pressure Product Industrial) equipped with a magnetic stirrer and Teflon liner. The polymerization temperature was controlled using a PID temperature controller (OMEGA, CN-8502) with a heating jacket and a cooling U-coil (water as coolant) inside the reactor. The temperature was measured using a thermocouple (OMEGA, K-type) immersed in a thermowell, connected to the temperature controller unit. During the reaction, the temperature was controlled within $\pm 1^\circ\text{C}$ of the set point. The rate of ethylene consumption was monitored by using a mass-flowmeter (Cole-Parmer, Model No.

32915-14) linked to a computer running LAB-VIEW v5.5 software.

Prior to each run, the reactor was dried at 150 °C under vacuum for 1 h. The temperature was cooled down while flushing with pure nitrogen for several times and ethylene for the last cycle. The stirring speed was constant at 1000 rpm. All chemicals made as solutions in toluene were packed into a cylindrical bomb under an inert atmosphere to transfer into the reactor by N₂ overpressure. First, 200 ml of toluene and a desirable amount of TIBA were added into the reactor to scavenge impurities. After stirring for 5 min, the operating temperature was set up to 40 °C. For the homogeneous system, a desired amount of zirconocene was loaded into the reactor and the reactor was pressurized with ethylene at 20 psig. The required amount of borane was loaded into the system to start the polymerization. In the heterogeneous system, after saturating the reactor at 20 psig of ethylene. (1) For the pre-activated metallocene systems: the prepared catalyst was directly charged into the reactor after adding TIBA; (2) in situ activated metallocene systems: zirconocene and B(C₆F₅)₃-SiO₂ were added separately into the system by injecting zirconocene followed by a desired amount of B(C₆F₅)₃-SiO₂. After 30 min, the reactor was cooled to room temperature and depressurized. A 10 ml of acidic-methanol was injected to quench the system. The final product was washed with excess methanol a few times, stirred in methanol overnight, filtered, and left in the hood for 4 days for complete drying and elimination of solvents.

2.4. Catalyst characterizations

The bulk concentration of boron (in B(C₆F₅)₃) on the silica support was determined by using inductively coupled plasma atomic emission spectrometer (ICP-AES Leeman Labs Plasma-Spec ICP Model 2.5). Samples for testing were prepared by digesting the catalyst powder in 4 N aqueous of HNO₃. A calibration curve was run prior to the samples and an independent check was run interspersed with the samples.

X-ray photoelectron spectroscopy (XPS, Perkin Elmer PHI 5400 model) was used to identify surface species as well determining the binding energy of electrons in the catalysts. The spectra were scanned at room temperature with a resolution of 0.1 eV in the range 0–800 eV. Samples were pressed to form pellets

under inert gas and then placed on the sample holder. The spectra of B (1s) at 151 eV and F (1s) at 690 eV were determined at 90° angle relative to the electron detector.

The interactions of boranes with the hydroxyls on the silica surface were investigated by FTIR spectroscopy (Mattson galaxy 7020 A model FTIR). The measurements were carried out under nitrogen atmosphere over the range 4000–2500 cm⁻¹. Samples were prepared by mixing catalyst powder with dried KBr, and then pressed into a pellet in a glove box.

The morphology of borane-supported catalysts was determined by scanning electron microscopy (SEM, Philips XL30 SEM). Due to the low electron emission samples, the sample must be sputtered and coated with carbon. Fluorine (F K) distribution was provided by using the energy-dispersed X-ray detector equipped with SEM and EDX control software.

2.5. Polymer characterizations

The average MWs and MWDs or polydispersity index (PDI) of polyethylene products were determined using a high-temperature gel permeation chromatography (GPC) equipped with three Water Ultrastayragel columns in series at 150 °C using *o*-dichlorobenzene as solvent. The columns were calibrated with narrow MWD polystyrene samples. The morphology of the polymer was investigated using an SEM (Philips XL30 SEM). The bulk density of the polymer particles was measured according to ASTM Standard D 1895.

3. Results and discussion

Fig. 1 shows the FTIR spectrum of silica before and after impregnation with borane compounds. There are many types of surface groups on the silica surface: single hydroxyl (i), hydrogen bound hydroxyls (ii), paired hydroxyls (iii) and adsorbed water (iv) [13]. Single silanol (Si-OH) groups result in a sharp peak at 3747 cm⁻¹ after calcination of silica at 500 °C. The broad band from 3400 to 3700 cm⁻¹ is assigned to interglobular OH groups retained inside the pore. Therefore, there are at least two different classes of surface silanols ready to complex with B(C₆F₅)₃. As evidenced by the absence of the single hydroxyl band of 3747 cm⁻¹, after the treatment with excess

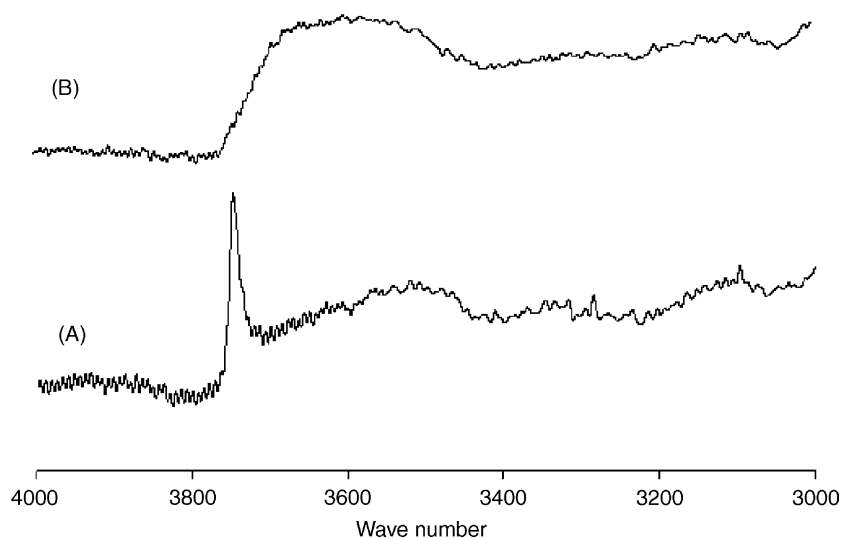


Fig. 1. FTIR spectra of borane supported on silica: (A) silica support at temperature 500 °C calcination; (B) $\text{SiO}_2\text{-B}(\text{C}_6\text{F}_5)_3$ catalyst. The sharp peak is due to isolated silanol group.

$\text{B}(\text{C}_6\text{F}_5)_3$, these hydroxyl groups (OH) appear to be totally converted to $-\text{OB}(\text{C}_6\text{F}_5)_3^-$ anions. However, a broad band at $3450\text{--}3750\text{ cm}^{-1}$ is still present at a reduced intensity after complexation, in agreement with Lancaster et al. [10]. We also quantitatively determined the amount of single hydroxyls that were converted to $-\text{B}(\text{C}_6\text{F}_5)_3^-$, based on the results of trimethyl aluminum titration only $\sim 15\%$ have been converted to $-\text{OB}(\text{C}_6\text{F}_5)_3^-$ anions. This result would imply that the FTIR is not detecting all of the isolated hydroxyls on silica.

Table 1 shows the comparison of preparation steps in terms of their effectiveness for loading $\text{B}(\text{C}_6\text{F}_5)_3$ on to the silica support as determined by ICP-AES.

Table 1
Adsorption of $\text{B}(\text{C}_6\text{F}_5)_3$ onto silica support

Code	Method of preparation ^a	B (mmol/g) ^b	Percent of borane deposited ^c	B:OH
BA	A	0.11	17	0.08
BB	B	0.22	35	0.15

^a Method A: stirring for 15 h in toluene and washing with toluene (4×5 ml); method B: stirring for 10 h in toluene and washing with toluene (3×5 ml) and hexane (2×5 ml); from this work.

^b From ICP-AES measurement.

^c Calculated from the original used amount of $\text{B}(\text{C}_6\text{F}_5)_3$.

Method B results in a borane concentration that is twice that of method A. This may be explained by noting that toluene has a higher efficiency than hexane to dissolve $\text{B}(\text{C}_6\text{F}_5)_3$ and remove it from the support surface in the washing step. Moreover, the measurement of $\text{B}(\text{C}_6\text{F}_5)_3$ adducted by OH group on silica showed higher B:OH ratio for method B than for method A. From these B:OH values, not all OH groups could be accessed by $\text{B}(\text{C}_6\text{F}_5)_3$. It may be suggested that the size of $(\text{C}_6\text{F}_5)_3$ group may prevent the penetration of $\text{B}(\text{C}_6\text{F}_5)_3$ into the pores of the silica support.

The XPS result shown in Fig. 2 is a representative survey spectra of borane supported on silica gel. All elements Si, O, C, B and F were detected. A weak peak due to Boron 1s is seen located at 151 eV and a strong peak of F 1s is presented at 686 eV. The presence of both elements verifies the existence of the borane compound on the surface, quantitative ratio of the peak areas gives the ratio of F:B $\sim 13.8:1$ (stoichiometric atoms of 15:1). The Si 2p spectrum consists of two peaks at 103.3 and 101.7 eV, which can be attributed to Si atoms in the bulk and at the surface.

The above results show that the use of $\text{B}(\text{C}_6\text{F}_5)_3$ lead to surface bound, silanol–borane adducts which activate alkylated zirconocene (e.g. Cp_2ZrMe_2 , Cp_2ZrBu_2) for ethylene polymerization. The hydroxyl

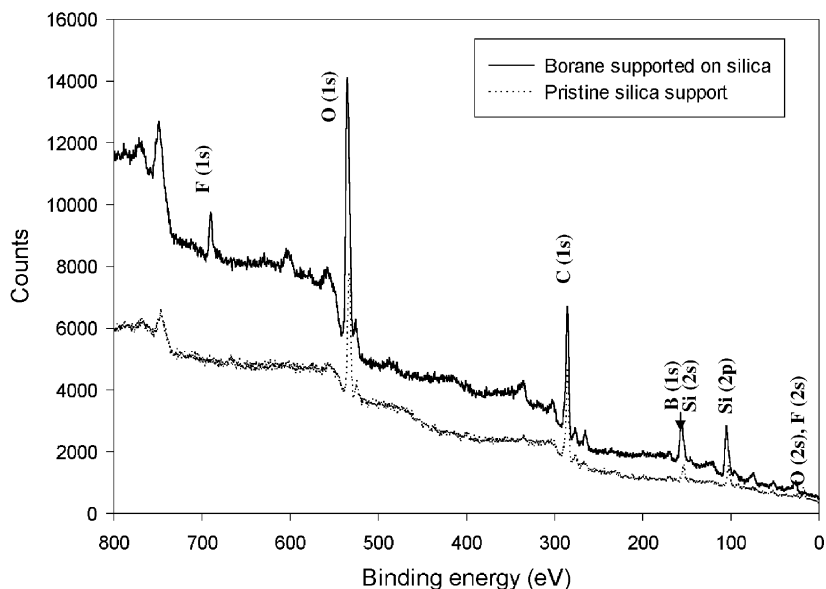


Fig. 2. XPS survey spectra of borane-supported indicated elements on silica surface (BB supported borane from Table 1).

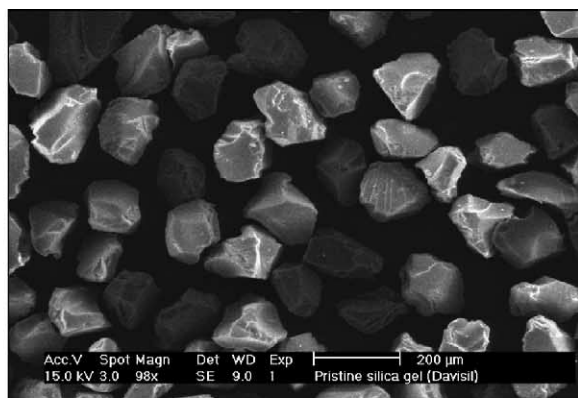
groups on the silica surface act as strong Lewis acids to create the anionic active species $-\text{OB}(\text{C}_6\text{F}_5)_3^-$ for generating cationic active species $[\text{Cp}_2\text{ZrR}]^+$ for either $\text{Cp}_2\text{ZrCl}_2/\text{TIBA}$ or Cp_2ZrMe_2 systems. Thus the supports act as polyanions to which the cationic active species are bound by electrostatic rather than covalent interactions [9,10].

SEM micrographs in Fig. 3(a) and (b) show the morphology of the pristine silica gel and the $\text{B}(\text{C}_6\text{F}_5)_3\text{-SiO}_2$ impregnated silica. It can be seen that the physical surface of silica gel after anchoring with $\text{B}(\text{C}_6\text{F}_5)_3$ is unchanged from the original morphology and diameter ($\sim 50 \mu\text{m}$). Fig. 3(c, left) shows an enlarged section of $\text{B}(\text{C}_6\text{F}_5)_3\text{-SiO}_2$. Fig. 3(c, right) shows the distribution of the fluorine atom on the same surface. The light patches are due to X-ray emission from the K-shell of fluorine (F K distribution map) of $\text{B}(\text{C}_6\text{F}_5)_3$ located on the silica surface. It is clear that the distribution is essentially random and uniform.

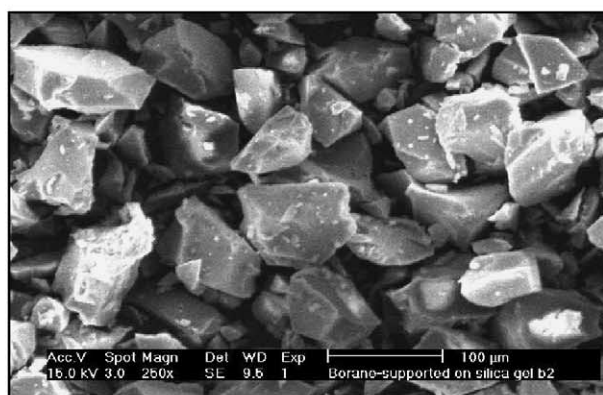
3.1. Activity of the catalyst systems

Ethylene consumption profiles provide important information about the activity and longevity of

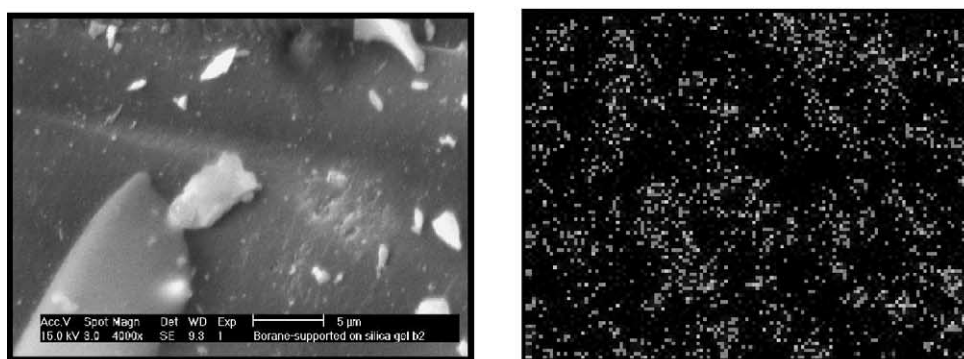
the catalysts [4–6]. Fig. 4 shows the ethylene consumption profiles of $\text{Cp}_2\text{ZrCl}_2/\text{TIBA}$ catalysts. The activity of the homogeneous system rises sharply and reaches its maximum of $\sim 210 \text{ cm}^3$ ethylene/min in 5 min after the injection of the catalyst into the reactor. The activity then decays in the next 5 min rapidly to $\sim 25\%$ of its peak activity. This rapid decay period is followed by a much slow decay with the activity decreasing to $\sim 30 \text{ cm}^3/\text{min}$ after 30 min. The pre-activated catalyst system also exhibits an initial rise in activity followed by a rapid decay and slow decay periods. However, the initial increase in rate is slower and the maximum is much lower ($\sim 60 \text{ cm}^3/\text{min}$) but the slow decay characteristics are almost identical with the homogeneous system. In comparison, the in situ activated catalyst system reaches its peak activity in the first 3 min ($\sim 60 \text{ cm}^3/\text{min}$). After a relatively slow decay to $\sim 45 \text{ cm}^3/\text{min}$ over the next 5 min, the activity stays constant at this level for the duration of the experiment. We repeated this experiment for a duration of 60 min and again did not see any decay in activity. A trace activity was exhibited in the system without additional TIBA. For in situ activated system with TIBA but one-tenth the supported borane amount



(a)



(b)



(c)

Fig. 3. SEM micrographs of (a) pristine silica support and (b) borane-supported catalyst. (c) An enlarged region of silica surface (left), fluorine mapping (F K) of borane on the same silica surface (right).

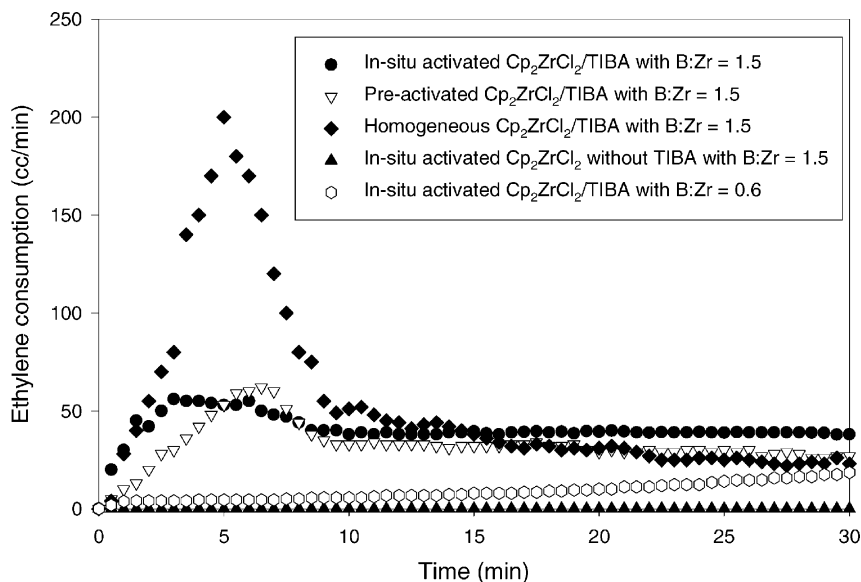


Fig. 4. Kinetic profiles of ethylene consumption during polymerization with different metallocene system: $[Zr] = 1.6 \mu\text{mol}$; $Al:Zr = 400$ (in case of desire); $B:Zr = 1.5:1$; $T_p = 40^\circ\text{C}$; ethylene = 20 psig.

($B:Zr = 0.6$), the activity increases slowly all the way to $25 \text{ cm}^3/\text{min}$ at the end of 30 min. We attribute this slow increase to activation of zirconocene by the supported co-catalyst.

The lack of long-term decay in the activity of the in situ activated catalyst system can be explained as being due an equilibrium reaction between the soluble metallocene left in solution and soluble $B(C_6F_5)_3$

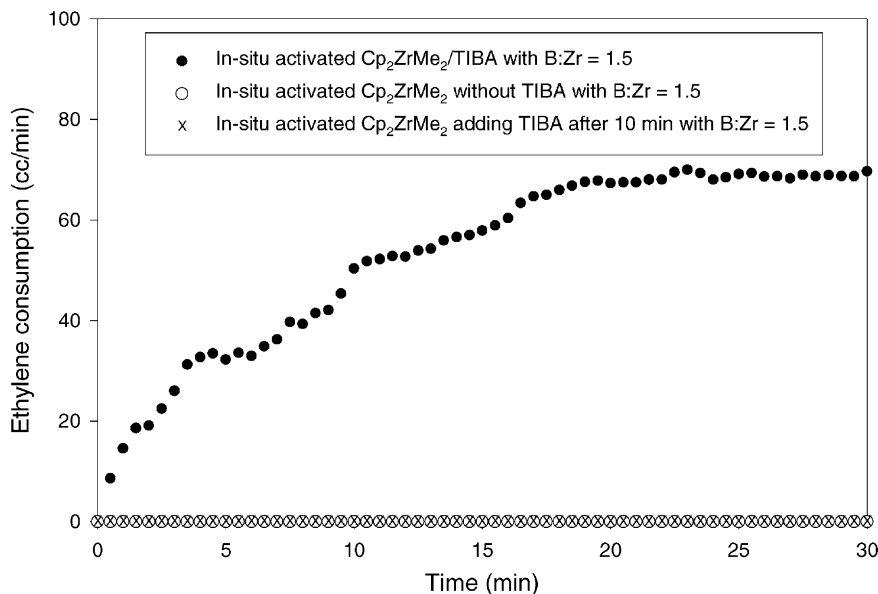


Fig. 5. Kinetic profiles of ethylene consumption during polymerization with in situ activated $Cp_2Zr(CH_3)_2$: $[Zr] = 19.1 \mu\text{mol}$; $Al:Zr = 50$ (in case of desire); $B:Zr = 1.5:1$; $T_p = 40^\circ\text{C}$; ethylene = 20 psig.

species, which exist in equilibrium with the surface bound metallocene and $B(C_6F_5)_3$ species. The species present in solution can create new active sites on the surface and compensate for the deactivation of the supported metallocene sites [4]. If this model is correct, we should see catalyst decay eventually because the reservoir of solution species will be exhausted. However, as mentioned above we did not see a decay even after extending the reaction period to 1 h at which time the amount of polymer in the reactor was too much to continue the reaction further.

In the case of in situ activated $Cp_2Zr(CH_3)_2 + B(C_6F_5)_3-SiO_2$ system, the ethylene consumption profile shown in Fig. 5 differs from the $Cp_2ZrCl_2/TIBA$ system, because there is no need for the alkylation step before reacting with $B(C_6F_5)_3$ on the support surface. The $B(C_6F_5)_3-SiO_2$ can directly react with $Cp_2Zr(CH_3)_2$ and create $Cp_2ZrCH_3^+$ active species for ethylene monomer insertion [14,15]. The activity increased slowly for the first 20 min and then stayed constant. This catalyst system showed good productivity only in the presence of TIBA in the system. In the absence of TIBA, the productivity was very low. Note that the data show the necessity of adding TIBA simultaneously with the catalyst.

However, the productivities of ethylene polymerization in both systems were much lower than their

analogous homogeneous systems. TIBA plays an important role to maintain the catalytic productivity by not only scavenging impurities of the system, but also being an alkylating agent for dichloro-zirconocene [16,17]. When this alkylated species reacts with $B(C_6F_5)_3-SiO_2$, it can produce metallocenium (*cationic-like*) species weakly coordinated to the anionic silica surface. When using $Cp_2Zr(CH_3)_2$, we found that much higher threshold concentrations of $Cp_2Zr(CH_3)_2$ are required when compared to the $Cp_2ZrCl_2/TIBA$ system. Ten minutes after adding TIBA, the productivity decreased to a very low value. This is most likely due to the degradation of dimethyl zirconocene, $Cp_2Zr(CH_3)_2$, by impurities and its low stability to storage or transfer [16]. Therefore, dichlorinated zirconocene is a much better catalyst. The use of TIBA for pre-alkylating Cp_2ZrCl_2 to generate the “bare” cation $[Cp_2ZrC_4H_9]^+$, and then activate with $B(C_6F_5)_3-SiO_2$ is more acceptable.

Due to Lewis acid character of the surface-functionalized ($-OB(C_6F_5)_3^-$) on silica support, it can form a non-coordinating anion with $[Cp_2ZrR]^+$ species [18–20]. CP MAS NMR results indicated that this non-coordinated $-OB(C_6F_5)_3^-Cp_2ZrR^+$ species has a highly reactive electrophilic, and unsaturated site, with “cation-like” character [14,15,21]. Therefore, the mechanism of the in situ activating metallocene system by $B(C_6F_5)_3-SiO_2$ can be proposed as

Table 2

The results of ethylene polymerization with metallocene/borane-supported system^a

Catalyst system	[Zr] (μmol)	B:Zr	A ₁ ^b	A ₂ ^c	Mw (×10 ⁻⁴)	Mw/Mn	Bulk density (g/ml)
Homogeneous ^d	1.68	1.5:1	8.70	–	13.2	3.2	0.041
Homogeneous ^d	1.68	1.5:1	8.94	–	15.4	3.1	0.048
Pre-activated (Cp_2ZrCl_2)	1.68	1.5:1	2.29	13	14.2	3.3	0.132
In situ activated (Cp_2ZrCl_2)	1.68	1.5:1	2.93	16	12.2	3.4	0.141
In situ activated (Cp_2ZrCl_2)	1.68	0.6:1	0.15	18	9.6	4.0	–
In situ activated (Cp_2ZrCl_2) ^e	1.68	1.5:1	Trace	–	–	–	–
In situ activated ($Cp_2Zr(CH_3)_2$)	19.1	1.5:1	0.43	37.5 ^d	15.4	6.4	0.133
In situ activated ($Cp_2Zr(CH_3)_2$) ^e	19.1	1.5:1	Trace	–	–	–	–
Pre-activated ($Cp_2Zr(CH_3)_2$) ^f	0.48 ^g	1:1	10.6	–	19.7	2.04	0.43

^a Polymerization conditions: toluene = 280 ml; T_p = 40 °C; TIBA = 1 mmol; ethylene = 20 psig; stirring speed = 1000 rpm; reaction time = 30 min.

^b Productivity (kg PE/(mmol Zr h atm)).

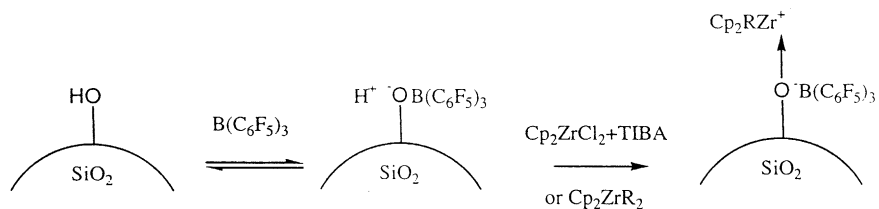
^c Productivity (g PE/(g support h atm)).

^d Homogeneous system: $Cp_2ZrCl_2/TIBA + B(C_6F_5)_3$.

^e Without adding TIBA.

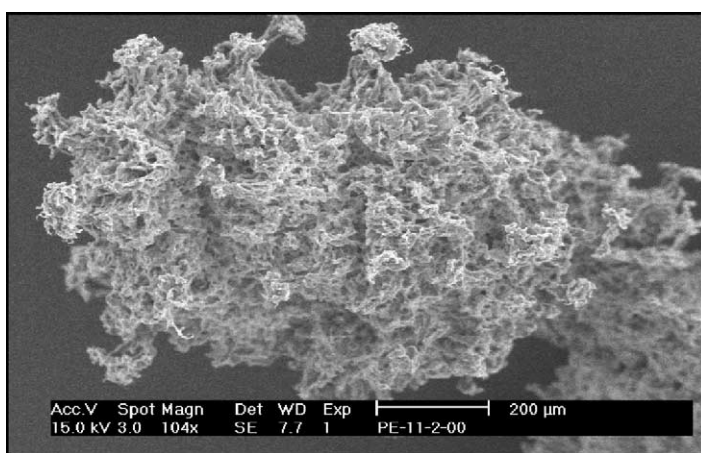
^f Polymerization condition: toluene = 500 ml; T_p = 70 °C; TIBA (Al:Zr = 10:1); ethylene = 75 psig; MAO:Zr = 50 [8].

^g mmol Zr/g supported catalyst.

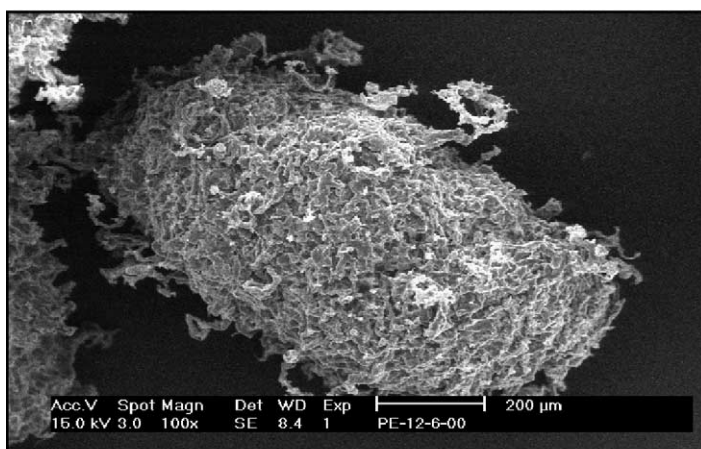


The MW and MWD of polyethylene produced from homogeneous, in situ activated and pre-activated metallocene systems were not significantly different and were in the range 120 000–150 000 for MW and 3–4 for MWD (see Table 2). We have also compared

our results with the previous results obtained with supported catalysts under different conditions. The bulk density of polyethylene from the in situ activated system was higher than the pre-activating metallocene system. Also the bulk densities in both systems



(a)



(b)

Fig. 6. SEM micrographs of polyethylene synthesized from (a) homogeneous metallocene system and (b) in situ activated metallocene/borane-supported system.

are much higher than the polyethylene from homogeneous system. However, there is essentially no difference between the in situ activated $\text{Cp}_2\text{ZrCl}_2/\text{TIBA}$ and $\text{Cp}_2\text{Zr}(\text{CH}_3)_2$ systems.

SEM micrographs in Fig. 6 show the morphology of polyethylene synthesized from the in situ activated metallocene systems and homogeneous systems. From the pictures, we can conclude that the in situ activated metallocene by supported borane gives polyethylene product with a good morphology. The polyethylene from the in situ activated metallocene system has lower porosity particles than that from the homogeneous system. The final size of polyethylene particles is about $500\ \mu\text{m}$ in diameter, larger than the original support by an order of magnitude and has an irregular surface. For the homogeneous system, the morphology of polymer particles is “spongy-like”.

4. Conclusions

The siloxane groups on activated silica support can react with $\text{B}(\text{C}_6\text{F}_5)_3$ to create anionic borato species $(-\text{OB}(\text{C}_6\text{F}_5)_3)^-$ when contacted with excess $\text{B}(\text{C}_6\text{F}_5)_3$ in toluene. This supported borane co-catalyst showed remarkable results in activating the metallocene catalyst in situ. Our study shows that this supported catalyst can be utilized for ethylene polymerization without additional aluminoxane compounds. However, TIBA is needed to activate this catalyst in the reactor. TIBA has the dual role of scavenging the impurities as well being the alkylating agent for dichlorinated zirconocene [22].

The in situ polymerization system has shown improvement of ethylene polymerization activity with supported borane co-catalysts. The in situ activated metallocene system showed better catalytic performance than pre-activated metallocene system in time scales up to 60 min. In case of in situ activated $\text{Cp}_2\text{ZrCl}_2/\text{TIBA}$ system, the activity is independent of time while the pre-activated $\text{Cp}_2\text{ZrCl}_2/\text{TIBA}$ system shows faster deactivation. MW and MWD for both pre-activated and in situ activated metallocene systems were not significantly different, but the bulk density was a factor of 3 and higher over that of the homogeneous system. In addition, both heterogeneous metallocene systems reduced the fouling and gave good morphology polymer product with high density.

Acknowledgements

The authors would like to acknowledge to Thai Polyethylene Co., Ltd., for GPC and bulk density analysis as well as providing a fellowship to S.C.

References

- [1] J.C.W. Chien, *Top. Catal.* 7 (1999) 23.
- [2] M.R. Ribeiro, A. Deffieux, M.F. Portela, *Ind. Eng. Chem. Res.* 36 (1997) 1224.
- [3] G.G. Hlatky, *Chem. Rev.* 100 (2000) 1347.
- [4] K.J. Chu, J.B.P. Soares, A. Penlidis, *J. Polym. Sci. A* 38 (2000) 462.
- [5] K.J. Chu, J.B.P. Soares, A. Penlidis, *Macromol. Chem. Phys.* 201 (2000) 552.
- [6] K.J. Chu, J.B.P. Soares, A. Penlidis, *J. Polym. Sci. A* 200 (1999) 2372.
- [7] E.Y.X. Chen, T.J. Marks, *Chem. Rev.* 100 (2000) 1391 and references therein.
- [8] J. Tian, S. Wang, Y. Feng, J. Li, S. Collins, *J. Mol. Catal. Chem.* 144 (1999) 137.
- [9] M. Bochmann, G. Jiménez Pindado, S.J. Lancaster, *J. Mol. Catal. Chem.* 146 (1999) 179.
- [10] S.J. Lancaster, S.M. O'Hara, M. Bochmann, in: W. Kaminsky (Ed.), *Metalorganic Catalysts for Synthesis and Polymerization*, Springer, Berlin, 1999, p. 413.
- [11] M.J. Carney, K.Y. Shih, in: *Proceedings of the Fifth International Congress on Metallocene Polymers, Metallocenes Europe'98*, p. 121.
- [12] S. Collins, W.M. Kelly, D.A. Holden, *Macromolecules* 25 (1992) 1780.
- [13] G. Fink, B. Steinmetz, J. Zechlin, C. Przybyla, B. Tesche, *Chem. Rev.* 100 (2000) 1377.
- [14] W.C. Finch, R.D. Gillespie, D. Hedden, T.J. Marks, *J. Am. Chem. Soc.* 112 (1990) 6221.
- [15] M. Jezequel, V. Dufaud, M.J. Ruiz-Garcia, F. Carrillo-Hermonsilla, U. Neugebauer, G.P. Niccolai, F. Lefebvre, F. Bayard, J. Corker, S. Fiddy, J. Evans, J.P. Broyer, J. Malinge, J.M. Basset, *J. Am. Chem. Soc.* 123 (2001) 3520.
- [16] J.C.W. Chien, W. Song, M.D. Rausch, *J. Polym. Sci. A* 32 (1994) 2387.
- [17] J.C.W. Chien, W. Song, M.D. Rausch, *Macromolecules* 26 (1993) 3239.
- [18] R. Duchateau, R.A. van Santen, G.P.A. Yap, *Organometallics* 19 (2000) 809.
- [19] R. Duchateau, H.C.L. Abbenhuis, R.A. van Santen, A. Meetsma, S.K.-H. Thiele, M.F.H. van Tol, *Organometallics* 17 (1998) 5663.
- [20] R. Duchateau, U. Cremer, R.J. Harmsen, S.I. Mohamud, H.C.L. Abbenhuis, R.A. van Santen, A. Meetsma, S.K.-H. Thiele, M.F.H. van Tol, M. Kranenburg, *Organometallics* 18 (1999) 5447.
- [21] C. Sishta, R.M. Hathorn, T.J. Marks, *J. Am. Chem. Soc.* 114 (1992) 1112.
- [22] A.N. Panin, T.A. Sukhova, N.M. Bravaya, *J. Polym. Sci. A* 39 (2001) 1901.